Economic model-predictive control of building heating systems using Backbone energy system modelling framework

Rasku, Topi; Lastusilta, Toni; Hasan, Ala; Ramesh, Rakesh; Kiviluoma, Juha

Published in:
Buildings

DOI:
10.3390/buildings13123089

Published: 12/12/2023

Document Version
Publisher's final version

buildings

MDPI

Article

Economic Model-Predictive Control of Building Heating Systems Using Backbone Energy System Modelling Framework

Topi Rasku *, Toni Lastusilta, Ala Hasan, Rakesh Ramesh and Juha Kiviluoma

VTT Technical Research Centre of Finland Ltd., P.O. Box 1000, FI-02044 VTT Espoo, Finland; toni.lastusilta@vtt.fi (T.L.); ala_hasan@hotmail.com (A.H.)
* Correspondence: topi.rasku@vtt.fi

Abstract: Accessing the demand-side management potential of the residential heating sector requires sophisticated control capable of predicting buildings' response to changes in heating and cooling power, e.g., model-predictive control. However, while studies exploring its impacts both for individual buildings as well as energy markets exist, building-level control in large-scale energy system models has not been properly examined. In this work, we demonstrate the feasibility of the open-source energy system modelling framework Backbone for simplified model-predictive control of buildings, helping address the above-mentioned research gap. Hourly rolling horizon optimisations were performed to minimise the costs of flexible heating and cooling electricity consumption for a modern Finnish detached house and an apartment block with ground-to-water heat pump systems for the years 2015–2022. Compared to a baseline using a constant electricity price signal, optimisation with hourly spot electricity market prices resulted in 3.1–17.5% yearly cost savings depending on the simulated year, agreeing with comparable literature. Furthermore, the length of the optimisation horizon was not found to have a significant impact on the results beyond 36 h. Overall, the simplified model-predictive control was observed to behave rationally, lending credence to the integration of simplified building models within large-scale energy system modelling frameworks.

Keywords: model-predictive control; building energy management; building energy flexibility; energy system modelling; energy system optimisation

Citation: Rasku, T.; Lastusilta, T.; Hasan, A.; Ramesh, R.; Kiviluoma, J. Economic Model-Predictive Control of Building Heating Systems Using Backbone Energy System Modelling Framework. *Buildings* **2023**, *13*, 3089. https://doi.org/10.3390/buildings13123089

Academic Editor: Adrian Pitts

Received: 1 November 2023
Revised: 28 November 2023
Accepted: 6 December 2023
Published: 12 December 2023

1. Introduction

Electrification of traditionally fossil-fuelled sectors such as transportation and heating is one of our more promising decarbonisation pathways. Unfortunately, most of our renewable electricity generation potential originates from variable sources, leaving power utilities scrambling for flexibility capable of mitigating said variability. This newfound demand for flexibility has rekindled interest in various demand-side management (DSM) measures as a potential alternative for investing in additional energy storage or dispatchable generation capacity.

Buildings are the largest consumers of energy worldwide, responsible for over 30% of the global final energy consumption [1] and expected to increase by around 30% in another twenty years [2]. Furthermore, heating, ventilation, and air conditioning (HVAC) systems maintaining comfortable indoor temperature conditions can account for more than 60% of a building's total energy consumption [3]. Thus, the heating and cooling sector holds significant DSM potential [4], but accessing it requires both sophisticated HVAC systems as well as control. While rule-based control can be effective in reducing energy consumption in buildings [5], it is incapable of properly accounting for the building's future thermal response. Model-predictive control (MPC) overcomes this issue, making it more suitable for harnessing the flexibility in buildings [6]. However, whether all this DSM potential will ever be realised is highly debatable, as factors such as economic and policy uncertainty, as well as the future development of national energy systems, all affect building owners' decisions to invest into advanced building HVAC systems.

On the level of individual buildings, MPC is typically employed for optimal control of the buildings' systems, often utilising detailed technical parameters or plentiful real-time measurements [7,8]. However, studying the impacts of such controls on energy-market scale makes holistically modelling each building infeasible and requires the use of dedicated energy system models. Furthermore, obtaining sufficient input data for detailed building models becomes increasingly more difficult as the scale or the modelled energy system increases, encouraging more simplified and robust modelling approaches. While there are studies examining the energy-system impacts of different power-to-heat measures [4], the integration of building-level and large scale energy system models is still not well understood.

The remainder of this paper is organised as follows: Section 1.1 summarises the relevant scientific background, while Section 1.2 highlights the contribution of this paper. The modelled buildings are detailed in Section 2.1, and the MPC implementation using the Backbone energy system modelling framework is explained in Section 2.2. Finally, the optimisation results are presented in Section 3, their implications are explored in Section 4, and conclusions are drawn in Section 5.

1.1. Background

While some features of MPC can be traced back as far as the 1950s, it did not see industrial applications until the mid-1970s with access to cheaper and more reliable computer-based control [9]. In modern-day society with near-ubiquitous computers, MPC has become appealing for smaller-scale applications as well, such as building HVAC control [7]. Furthermore, MPC has been successfully employed for building HVAC systems to reduce energy demand and costs, as well as increase the self-consumption of on-site renewables, all while satisfying the occupants' comfort [10,11]. The existing literature on building-level MPC is vast, as evidenced by the recent reviews by Drgoňa et al. [7], Yao and Shektar [10], and Taheri et al. [11]. Examples of economic MPC studies include a small residential building with a heat pump system with floor heating depicted using a third-order resistance-capacitance (RC) model [12], a multi-zone commercial building with variable air volume cooling systems modelled using EnergyPlus with controls optimised using MATLAB [13], real-world multi-objective MPC trials for commercial buildings in Australia [14], a single-family house with multiple local renewable energy systems [15], as well as a small energy community of four single-family houses [16]. City-scale economic scheduling studies have also been performed, e.g., for Copenhagen [17] and Helsinki [18], although focusing more on the district heating system than the buildings themselves. Recent advances in machine learning have also increased interest in data-driven predictive control for building applications [8].

All of the above-mentioned studies model buildings or cities strictly as "price-takers", meaning that any change in their energy consumption is assumed not to affect the operation of the overarching energy system and the balance of the spot energy markets. While this is true for current day-ahead spot electricity markets, if DSM by flexible buildings becomes mainstream and significant numbers of buildings begin shifting their consumption in unison, markets will be forced to account for the reacting demand in some manner. Thus, there have been several studies examining the widespread impacts of building-level flexibility on the energy-market-scale as well [4]. Most noteworthy among them are perhaps the studies by Hedegaard et al. [19,20], pioneering the integration of simplified building RC models with the large-scale energy system model Balmorel for studying investments into flexible residential heat pump systems for wind power integration. Similar approaches have since been applied for studying peak-net demand increase caused by electrification of heating via heat pumps in the UK [21], impact of market penetration of electric heating demand response in Belgium [22] and Finland [23], comparing different flexible heating technologies in Germany [24], as well as impacts of pan-European multi-flexibility-source load-shifting [25].

1.2. Contribution

Despite the wealth of studies on the subject of building-level MPC and its implications for energy system operations discussed in the previous section, to the authors' best knowledge, there has never been an attempt to examine whether the building models employed within large-scale energy system modelling frameworks can perform reasonable building-level MPC. While the results of the previous energy-system-scale studies have not indicated reasons to doubt the used approach, performing building-level simulations helps further validate it, as well as better understand its limitations. Thus, this paper aims to address this research gap by demonstrating that Backbone can capture the key dynamics of such control and briefly investigates the impact of different rolling horizon optimisation parameters on the results. This is a missing stepping stone toward system-level studies, where large-scale scenario analysis is supplemented by more detailed local-level modelling, helping improve the reliability of the results and possibly correct large-scale models through iterative approaches. Furthermore, the investment optimisation capabilities present in many large-scale energy system optimisation frameworks facilitate comparing the economic viability of widespread building-level DSM solutions against competing flexibility options on national scales.

2. Materials and Methods

A significant share of existing large-scale energy system modelling frameworks are based on mixed-integer linear programming (MILP), as concurrent solvers can efficiently handle very large problems [26]. This severely limits applicable building modelling options, however, as most detailed physics-based white-box models cannot be integrated directly due to their reliance on non-linear functions [27]. Similarly, data-driven black-box models typically employ mathematical frameworks that cannot be implemented in a MILP-compatible manner [8]. Fortunately, simplified grey-box RC-modelling approaches have been shown to sufficiently capture the temperature dynamics in buildings and can be integrated directly into MILP problems [28]. Although, while RC models are ideal for large-scale energy system model integration, detailed white-box models or data-driven black-box models typically perform better in terms of accuracy, reliability, and adaptability when it comes to building-level MPC applications with access to detailed technical properties and measurement data from the building [7,8].

The remainder of this section is organised as follows: Section 2.1 first presents the modelled buildings as well as a brief overview of the simplified RC model, before Section 2.2 introduces the key aspects of Backbone used for the MPC. Furthermore, the raw data and the code for processing the data for the case study have been made available through Zenodo for interested readers [29].

2.1. Modelled Buildings

Residential buildings make up most of existing building stocks, and as such, are of key interest for building MPC. In terms of the flexibility in space heating demand, the effective thermal mass of the building is a potentially important factor. Thus, this work included both a light wooden-framed detached house (DH) and a heavy concrete apartment block (AB), illustrated in Figure 1 and described in more detail in Tables 1 and 2, respectively. The modelled buildings were based on the readily made example buildings from the IDA ESBO v1.13 [30] simulation tool, adhering to the 2012 Finnish regulations [31]. However, ventilation heat recovery units were disabled for simplicity, as well as to keep the building models identical to the previous IDA ESBO validations [32].

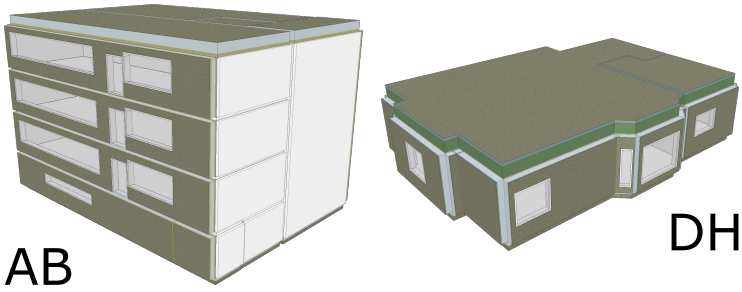

Figure 1. Illustrations of the modelled apartment block (AB) and detached house (DH). Note that the shown IDA ESBO model for AB represents only one half of the entire building and is mirrored over the partition walls shown in light grey to form the full building.

Table 1. Key properties of the modelled detached house (DH).

Gross floor area	135.56 m^2
Number of storeys	1
Room height	2.6 m
Ventilation air change rate	0.55 times per hour
Infiltration air change rate	0.06 times per hour
Window U-value	1.0 W/m^2K
Window solar heat gain coefficient	0.55
Window-to-wall ratio	0.20

Structure	Description	U [W/m^2K]	C_{eff} [kJ/m^2K]
Roof	13 mm plasterboard finish, 482 mm mineral wool insulation, asphalt roll roofing.	0.09	21.96
Exterior wall	13 mm plasterboard finish, 237 mm mineral wool insulation, 20 mm board exterior.	0.17	15.61
Base floor	20 mm autoclaved aerated concrete finish, 200 mm concrete slab, 207 mm expanded polystyrene insulation.	0.18	487.49
Partition wall	Timber frame, 13 mm plasterboard finish on both sides.	—	18.28

Table 2. Key properties of the modelled apartment block (AB).

Gross floor area	1608.19 m^2
Number of storeys	4 (counting the basement)
Room height	2.7 m
Ventilation air change rate	0.67 times per hour
Infiltration air change rate	0.04 times per hour
Window U-value	1.0 W/m^2K
Window solar heat gain coefficient	0.55
Window-to-wall ratio	0.26

Structure	Description	U [W/m^2K]	C_{eff} [kJ/m^2K]
Roof	10 mm mortar finish, 150 mm concrete slab, 486 mm mineral wool insulation, asphalt roll roofing.	0.09	412.71
Exterior wall	10 mm mortar finish, two 100 mm concrete slabs sandwiching 252 mm mineral wool insulation.	0.17	263.25
Base floor	20 mm autoclaved aerated concrete finish, 200 mm concrete slab, 207 mm expanded polystyrene insulation.	0.18	487.49
Partition wall	160 mm concrete slab.	—	375.28
Separating floor	20 mm autoclaved aerated concrete finish, 150 mm concrete slab.	—	334.34

The IDA ESBO building models were reduced into simplified RC models with only three temperature nodes depicting each building, namely the indoor air and furniture node, and the heavy and light structural mass nodes, illustrated in Figure 2. This nodal configuration had the most robust performance in terms of uncertainties related to the structural and solar gain properties in previous IDA ESBO validations [32], and the same RC models were reused in this work with the addition of a domestic hot water (DHW) tank temperature node to represent its storage capacity. A summary of the key indicators used for validating the RC models against IDA ESBO is presented in Table 3. For the sake of brevity, the RC model validation is not reproduced here, and interested readers are instead kindly referred to the aforementioned previous work [32]. While more accurate RC models could undoubtedly be obtained via state-of-the-art calibration routines [33] and processed for Backbone, these robust models were chosen for this demonstration as they better represent the intended use case on the energy-system scale, where detailed measurement or simulation data for proper calibration are often lacking. The indoor air and DHW tank node temperatures were constrained between 21 and 25 °C and 60 and 90 °C, respectively, based on the Finnish building code [34,35], governing the available flexibility in space and water heating demands.

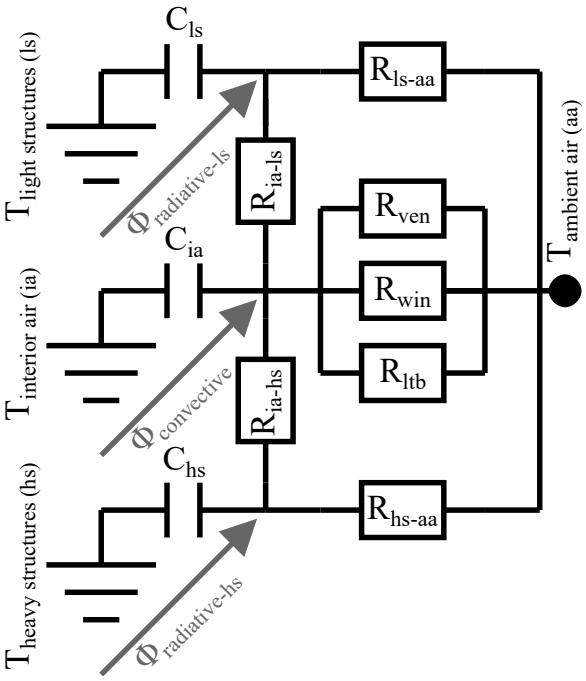

Figure 2. The resistance–capacitance model for the buildings. *C* denotes effective thermal masses of the model nodes, *R* represents the thermal resistances between the nodes, and Φ indicates the impact of solar and internal heat gains, as well as radiative sky losses. The interior air (ia) is directly in contact with ambient air (aa) via ventilation (ven), the windows (win), and the linear thermal bridges (ltb) through the envelope structures.

Table 3. Summary of the key indicators for the full-year free gross-floor-area-averaged indoor air temperature comparisons with IDA ESBO performed in [32] for the used RC models.

Indicator	Detached House (DH)	Apartment Block (AB)
Root-mean-square error [°C]	0.286	0.378
Maximum overestimation [°C]	1.23	1.48
Maximum underestimation [°C]	−0.937	−0.671

Time-varying prices make the use of economic MPC more worthwhile, so the buildings were modelled with ground-to-water heat pump (G2WHP) systems for both space and wa-

ter heating. For simplicity, the G2WHP was modelled using a simple seasonal performance factor (SPF) of 2.5, as suggested by Finnish building code calculation guides for G2WHPs with 60 °C hydronic radiator heat distribution systems typical in Finland [36]. Similarly, the buildings were equipped with ground-source cooling systems with SPF of 30 [36] to ensure feasible indoor air temperatures during summer. While temperature-dependent coefficients of performance for the heat pumps could be used to improve the accuracy of the modelling, they were purposefully avoided in order to permit calculating a more realistic baseline using Backbone, as explained in Section 3.1. The heating and cooling systems were assumed to be sized such that they could handle all heating and cooling demand in the modelled buildings without the need of auxiliary systems.

The G2WHP was also used for pre-heating DHW up to 60 °C, but topping up to the maximum 90 °C permitted for the modelled DHW tanks using resistance heaters reduced the overall SPF to ≈ 1.58. The DHW storage tanks were sized to store roughly two-thirds of the assumed daily DHW demand with the permitted temperature range, resulting in 250 and 3000 L tanks for the modelled detached house and apartment block, respectively. The sizing, heat losses, and other relevant technical properties of the DHW tanks were based on typical values presented in the Finnish building code calculation guides [35]. It is worth noting that the heat losses from the DHW tanks were assumed to be fully utilisable, contributing to the internal heat gains. While this is not often the case in reality, it simplifies the model and is sufficient for the purpose of this paper.

The internal heat gains and DHW demand profiles were based on simple typical daily profiles in the national calculation guides [35] presented in Figure 3. The internal heat gains include the assumed effect of inhabitants, appliances, and lighting but were aggregated into a single total heat gain profile for simplicity. Using identical profiles for both the modelled detached house (DH) and apartment block (AB) is not ideal, as the profiles are dependent on the building type in reality. However, the identical profiles are acceptable for the purpose of this paper. Meanwhile, the ambient temperatures, solar heat gains, and radiative sky losses were processed using ArchetypeBuildingModel.jl [37] and PyPSA/atlite [38] based on weather data from the ERA5 global reanalysis dataset [39] for the coordinates of the Helsinki-Vantaa airport.

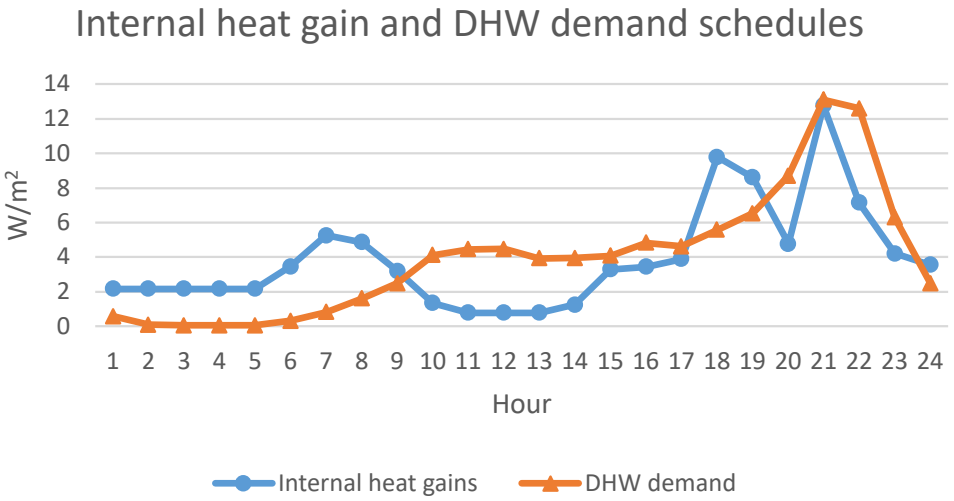

Figure 3. Assumed daily schedules of internal heat gains and as domestic hot water demand [35].

2.2. Backbone MPC Implementation

Backbone is an open-source MILP-based large-scale energy system modelling framework written in GAMS, primarily developed for solving expansion planning, hydro-thermal scheduling, and unit commitment problems. In order to accommodate such a broad scope of problems, the temporal, stochastic, and system depictions were designed in a generic and adaptable manner, allowing users to define radically different problems via input data

and definitions. Here, only the key aspects of Backbone relevant for building-level MPC are presented, and readers interested in further details are kindly referred to the paper by Helistö et al. [40] containing the full model formulation.

At its core, Backbone is a cost minimisation model, where the objective function depicts the total system costs of generating all the energy required to satisfy the demand in the modelled system, as well as installing new or replacing old assets. As such, Backbone is primarily suited for economic MPC of buildings, although other objectives could also be accommodated either by pricing them in the objective function or by introducing custom constraints to the problem. In this work, Backbone was configured to perform rolling horizon economic optimisation depicting MPC, and it is important to understand the following distinctions going forward:

Time step t refers to the time indices of the model, and Δ_t refers to the length of time step t in hours. In this work, only hourly time resolution was used $\Delta_t = 1\,\text{h}\;\forall t$.

Optimisation interval refers to the frequency of the rolling horizon optimisation, e.g., a 6 h interval meant that results were saved for the first six hours of each solve, before moving forward by six hours for the next solve.

Optimisation horizon $\mathbb{T}$ refers to the set of time steps t in each solve, e.g., with a 36 h horizon, optimal control was always solved for the next 36 h before rolling.

The key costs for building-scale MPC typically only include the costs of imported energy, reducing the simplified MPC optimisation problem to the following:

$$\begin{aligned}
&\text{Find a vector} && v \\
&\text{that minimises} && \sum_{t\in\mathbb{T}}\sum_{u\in\mathbb{U}}\left[\tau^{\text{ts_price}}_{import,t}\, v^{\text{gen}}_{import,u,t}\,\Delta_t\right] && (1)\\
&\text{subject to} && \frac{p_n^{\text{energyStoredPerUnitOfState}}}{\Delta_t}\left(v^{\text{state}}_{n,t} - v^{\text{state}}_{n,t-\Delta_t}\right) \\
& && \quad = -p_n^{\text{selfDischargeLoss}}\, v^{\text{state}}_{n,t} - \sum_{n'\in\mathbb{N}_n}\left[p^{\text{diffCoeff}}_{n,n'}\left(v^{\text{state}}_{n,t} - v^{\text{state}}_{n',t}\right)\right] \\
& && \quad + \sum_{u\in\mathbb{U}_n}\left[v^{\text{gen}}_{n,u,t}\right] + \tau^{\text{influx}}_{n,t} \qquad \forall\, n\in\mathbb{N}, t\in\mathbb{T} && (2)\\
& && v^{\text{gen}}_{import,u,t} = p_u^{\text{slope}}\, v^{\text{gen}}_{n,u,t} \qquad \forall\, u\in\mathbb{U}, n\in\mathbb{N}_u, t\in\mathbb{T}, && (3)\\
&\text{and} && p_n^{\text{downwardLimit}} \le v^{\text{state}}_{n,t} \le p_n^{\text{upwardLimit}} \qquad \forall\, n\in\mathbb{N}, t\in\mathbb{T}, && (4)\\
& && 0 \le v^{\text{gen}}_{import,u,t} \le p^{\text{capacity}}_{import,u} \qquad \forall\, u\in\mathbb{U}, n\in\mathbb{N}_u, t\in\mathbb{T}, && (5)
\end{aligned}$$

where p, v, and τ denote different parameters, variables, and time series, respectively, with their names indicated by the superscript and indices by the subscript. By exploiting Backbone's generic design, its energy networks can be parameterised to represent building RC models as illustrated in Figure 4. The set $\mathbb{U}$ contains all heating and cooling equipment units u, and the set $\mathbb{N}$ contains all the temperature nodes shown in the same figure. The objective function in Equation (1) is relatively straightforward, representing the total cost of imported electricity for all units $u \in \mathbb{U}$ and over the entire optimisation horizon $t \in \mathbb{T}$, where *ts_price* is the electricity price time series in €/Wh, and the *gen* variable represents the electricity consumed in W by the heating and cooling units. Please note that Equations (1)–(5) have been considerably simplified from the full Backbone formulation [40], omitting unused features such as controlled energy transfer and spill variables, variable and fixed costs related to units and energy transfer, capacity expansion related investment costs and discount factors, as well as forecast and scenario indices and their weights.

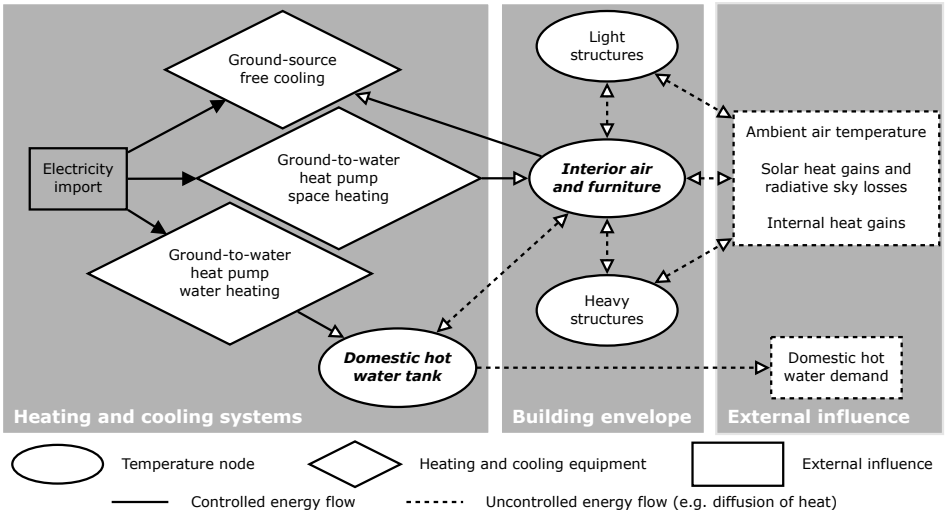

Figure 4. Energy system structure for the modelled buildings. Essentially, the MPC minimises electricity import costs of the heating and cooling systems while maintaining acceptable building node temperatures under changing weather, heat load, and heat demand conditions.

When implementing simple building RC models within Backbone via the energy balance constraint in Equation (2), the *state* variables represent the temperature of the building nodes in K, the *energyCapacity* parameter depicts the heat capacity of said nodes in Wh/K, while the *diffCoeff* determines the heat transfer coefficients between them in W/K. The heating equipment are depicted simply using the *gen* [W] variables, either adding energy when heating or removing energy when cooling. Here, the subsets $\mathbb{N}_n$ and $\mathbb{U}_n$ are used to indicate which nodes n' and units u are connected to the energy balance on the current node n, as illustrated by Figure 4. Unfortunately, Backbone does not have dedicated parameters for supporting building-specific interactions such as heat losses into the ambient air, solar gains, or internal heat gains in Equation (2), requiring them to be pre-processed to fit into Backbone's data structure. The ambient temperature interaction can be separated into its indoor-air and ambient-air-temperature-dependent constituents and implemented via a combination of the *selfDischargeLoss* [W/K] parameter and the *influx* [W] time series. Similarly, since solar and internal heat gains are assumed independent of the variables, their effects can be added to the *influx* time series as well. For readers interested in further details on the building RC model processing for Backbone, please refer to the ArchetypeBuildingModel.jl online documentation [37].

The energy conversion constraint in Equation (3) governs the operation of the heating and cooling units $u \in \mathbb{U}$, namely the G2WHP and ground-source cooling, by enforcing a fixed ratio between the input and output energy of each unit. In Backbone, the *slope* parameter represents the heat rate of unit u, which is the inverse of its efficiency, or the SPF in our case. Here, it is worth noting that space heating and water heating using the G2WHP are treated as independent units as shown in Figure 4 for simplicity. Furthermore, since the ground-source cooling system unit is removing heat from the indoor air node, its *slope* parameter and thus also its *gen* variable are negative.

Equation (4) sets the bounds for the *state* variables between the given *lowerLimit* [K] and *upperLimit* [K] parameter values. While all of the temperature nodes presented in Figure 4 were constrained for computational reasons, the limits for the light and heavy structure nodes were set loose enough not to impact the operation of the MPC, leaving the interior air and DHW tank temperature limits discussed in Section 2.1 to govern the flexibility available to the MPC. Similarly, Equation (5) sets the upper bounds for the electricity import *gen* variables via the *capacity* [W] parameters based on the assumed system sizing discussed in Section 2.1.

For the simulations presented in Section 3, Backbone was configured to perform 8736 h rolling horizon optimisations depicting the MPC of the modelled buildings. Essentially,

the MPC optimisation problem presented in Equations (1)–(5) was solved for the desired optimisation horizon $\mathbb{T}$, the resulting optimal values for the *state* and *gen* variables were fixed for the chosen optimisation interval, and the problem was rolled forward by the interval to be resolved for the next horizon. In order for the rolling horizon optimisation to obtain results for the last hours of the simulation, the horizon can extend beyond the current year. Backbone deals with this by recycling data from the beginning of the year to make up for the missing information, which can result in unrealistic swings in electricity prices and ambient conditions. Thus, the length of the simulations was limited to 8736 h to avoid "overshooting" the year when using a 168 h optimisation interval, as well as to mitigate any potential impacts of the end of the year on the results.

3. Results

In order to demonstrate that the Backbone energy system modelling framework can capture the essence of simplified building-level MPC, simulations were performed both using constant and time-varying hourly spot electricity prices for the years 2015–2022 as the control signal. Multiple recent years were simulated in order to examine the fluctuations in cost savings between years. The simulations using the constant electricity prices served as a baseline to compare the spot price simulations against, allowing us to ensure the MPC behaved logically with the given objective. The main results are presented in Section 3.1, while Section 3.2 presents further results with longer optimisation intervals and horizons in order to analyse their impact on the main results.

Electricity spot market prices were obtained from ENTSO-E [41], but in order to arrive at more realistic consumer prices, electricity taxes of 22.53 €/MWh for Finnish residential consumers [42] and an assumed profit margin of 2.40 €/MWh were included. For the baseline simulations, yearly average prices were used as the control signal in the objective function, but the final cost values were calculated using the resulting hourly electricity consumption and the hourly spot market prices in order to keep the costs comparable.

Perfect information about future electricity prices and weather conditions were assumed, regardless of the used optimisation horizon. While Backbone could solve rolling horizon optimisation with a single forecast or even stochastic forecasts, these were omitted for simplicity and to keep the focus on model performance. All of the simulations were performed on a laptop with an *11th Gen Intel(R) Core(TM) i7-1185G7 @ 3.00 GHz (4 cores)* processor and 32 GB of RAM, using Cbc [43] to solve the rolling horizon optimisation problems generated by Backbone.

3.1. MPC Cost Savings

The main MPC simulations employed 12 h rolling horizon optimisation solved every hour, representing a horizon for which the prices are always known in current day-ahead markets. Figure 5 presents an overview of the MPC behaviour for the year 2022 when provided with both constant and hourly spot electricity prices as the control signal. As seen in Figure 5a, the MPC had no incentive to utilise the available flexibility given constant electricity prices, thus expending the least amount of effort to maintain permitted node temperatures. Essentially, the MPC behaved as intended, enabling its use as the baseline for the spot electricity price simulations. However, it is worth noting that this baseline is noticeably more energy efficient than what more traditional control schemes could achieve. Furthermore, the baseline can be calculated in this manner only thanks to the simplifying assumption of a fixed SPF for the G2WHP systems. Otherwise, Backbone would exploit the flexibility in heating and cooling demand to shift heat pump consumption towards hours with better coefficients of performance, making the baseline unreasonable for the intended comparisons. Meanwhile, Figure 5b using spot electricity prices shows the MPC taking advantage of the available flexibility, as the DHW tank and interior air node temperatures can be seen to vary throughout the year. The full-year results are only presented for the detached house, as there is little visible difference in the overall behaviour of the apartment block.

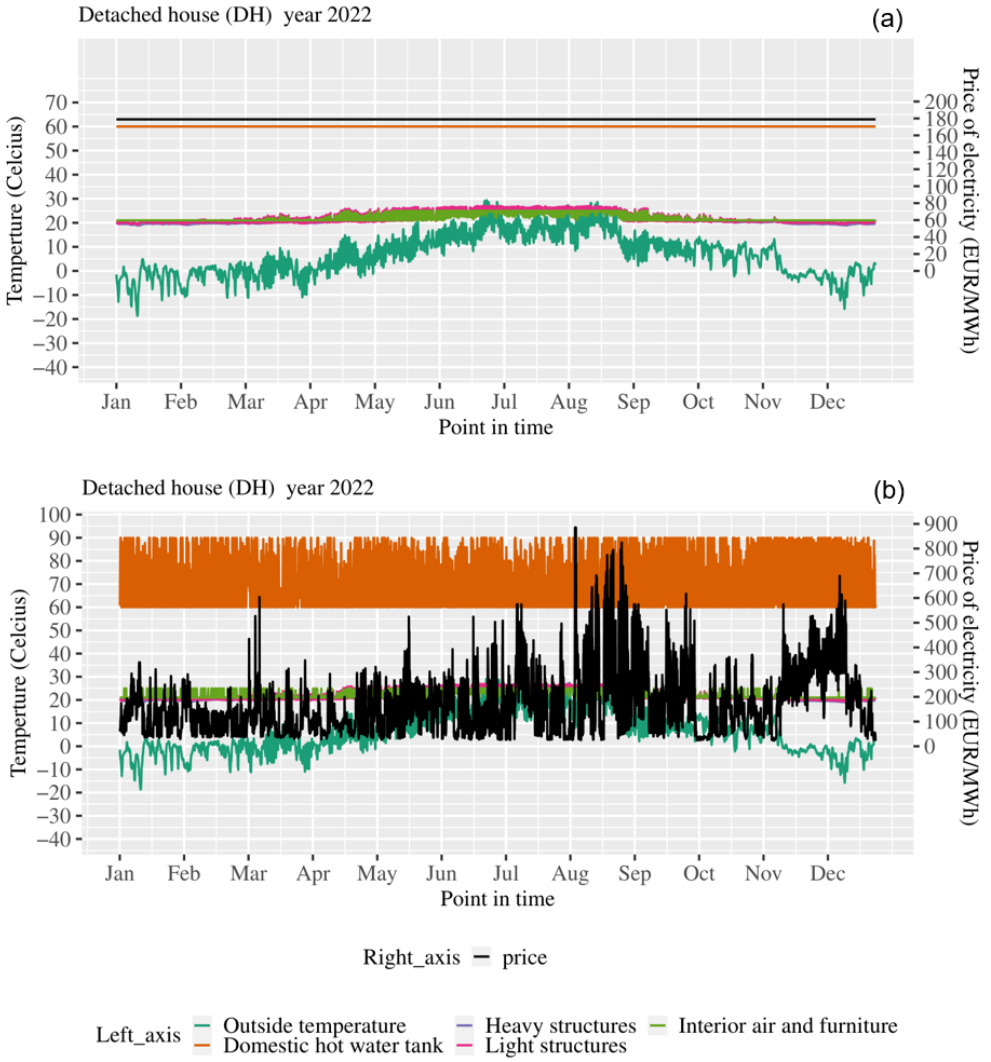

Figure 5. An overview of the full-year detached house simulation results using constant (**a**) and spot (**b**) electricity price control signals for the year 2022. With constant electricity prices (**a**), the MPC has no incentive to utilise the available flexibility and focuses on simply maintaining acceptable temperatures throughout the year. The constant price simulation in (**a**) is used as the baseline for comparing the savings achieved by the spot price simulation in (**b**).

Figure 6 presents a more detailed view of the MPC operation of the spot electricity price simulations during one week in February 2022. The DHW tank can be seen charging mostly during the cheaper hours of the night, with some extra heating during comparatively cheap hours during the day as well. Since both buildings had the same typical DHW demand profile, the DHW tanks were utilised in near-identical manner, which can also be observed for the full-year-duration curve presented in Figure 7b. On the other hand, the space heating system can be seen overheating the interior air only before sharp increases in electricity prices. Curiously, comparing the space heating system operation for DH and AB in Figure 6, the DH can be seen to utilise its flexibility slightly more often. Figure 7a similarly shows a larger difference between the interior air node temperature of the DH compared to the AB throughout the year, corroborating the previous observation. Interestingly, the AB also utilised its space cooling flexibility enough to reduce the number of high-temperature hours inside the building.

Table 4 presents a summary of the key results from the simulations, focusing on comparing the performance of the spot electricity price-optimised MPC against the baseline. The total yearly heating and cooling costs ranged between 417 and 1477 € for the DH and between 4049 and 14,252 € for the AB depending on the modelled year, with yearly savings ranging between 17 and 269 € (3.1–15.4%) and 196 and 3020 € (3.6–17.5%) for the DH and AB, respectively. However, the yearly energy consumption compared to the baseline was slightly increased by around 1.1–3.0% for the DH and around 1.3–2.8% for the AB due to the additional heat losses caused by utilising the heat storage capacity in the building. The DHW tank was found to be responsible for the majority of the cost savings, ranging from 70.4 to 83.4% and 74.1 to 88.0% of the savings for the DH and AB, respectively, depending on the simulated year.

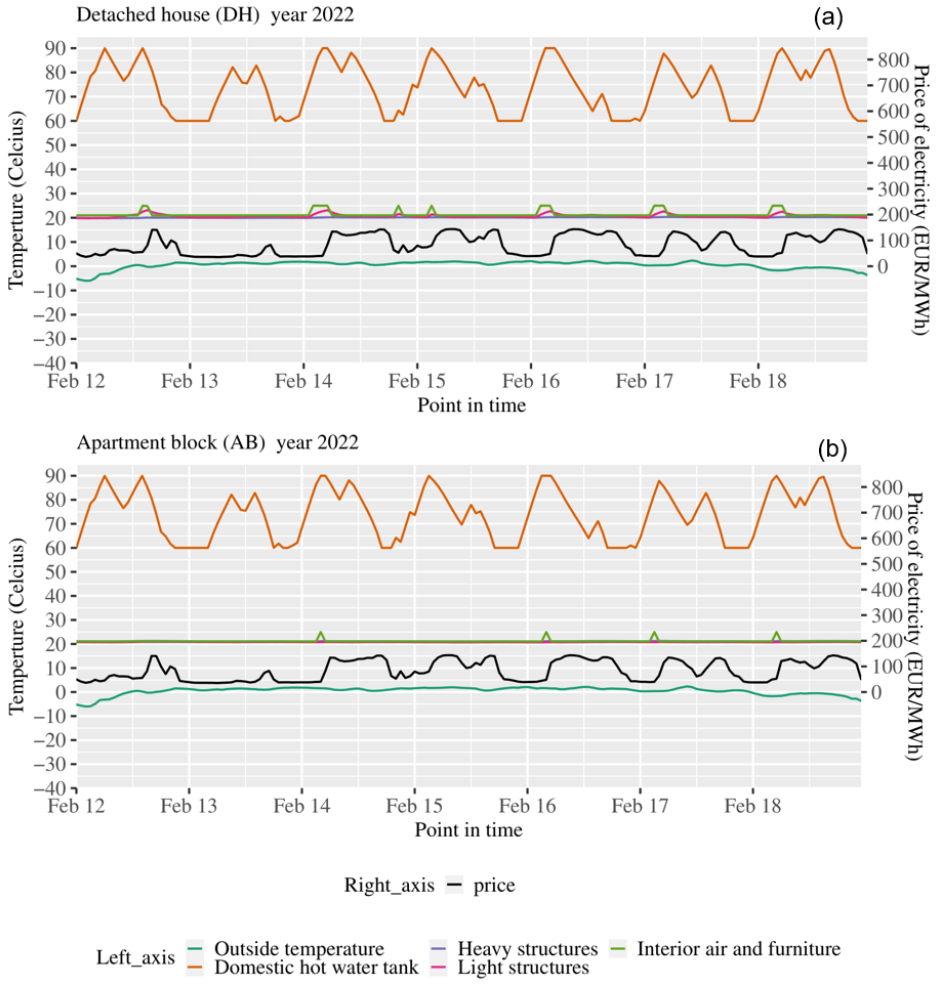

Figure 6. Example spot price optimisation results for week 7 in 2022 for the DH (**a**) and AB (**b**), respectively. The domestic hot water tank and interior air and furniture node temperatures are charged when electricity prices are low to reduce electricity consumption during more expensive hours, reducing costs.

The yearly fluctuations in the DHW share of savings were at least partially due to the yearly variations in space heating demand presented in Tables 5 and 6, driven by the heating degree days (HDD), as shown in Figure 8. During colder years with more HDDs, the space heating demand increases, which in turn seemed to allow more flexibility from the space heating system. Meanwhile, the flexibility available from the DHW demand was essentially identical between the years, resulting in the DHW share of savings fluctuating between the years. Fluctuating electricity prices also play a part in determining the DHW share of savings, but due to the complex dependencies between electricity prices, weather

conditions, and the properties of space and water heating flexibility, their impacts are extremely difficult to analyse.

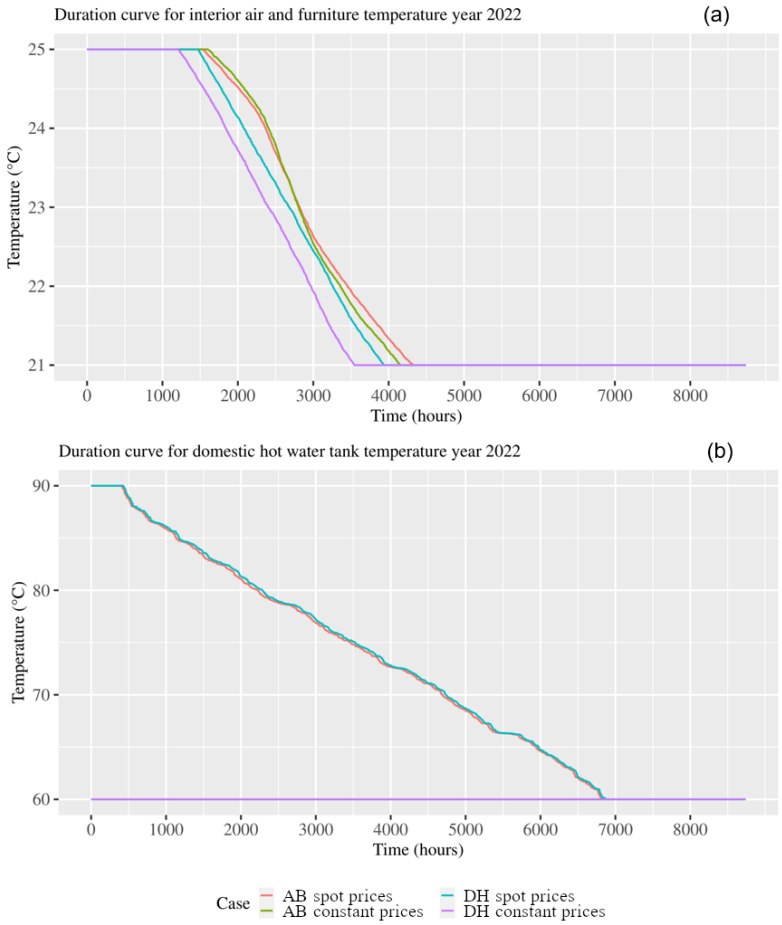

Figure 7. Duration curves for interior air and furniture temperature (**a**) and domestic hot water tank temperature (**b**) in 2022. Both AB and DH can be seen to have higher indoor air and DHW tank temperatures throughout most of the year with spot prices, as heat is stored into the building during cheaper hours. Note that in (**b**), the *AB constant prices* overlap with the *DH constant prices*, as neither had any incentive to charge the DHW tank temperature in the constant price baseline.

Table 4. Key yearly results for 2015–2022, hourly optimisation interval, and 12 h horizon.

Detached house (DH)	**2015**	**2016**	**2017**	**2018**	**2019**	**2020**	**2021**	**2022**
Baseline consumption [kWh]	8775	9782	9451	9732	9353	8518	9988	9418
MPC consumption [kWh]	8901	9902	9552	9836	9478	8691	10,188	9699
— Increase [kWh]	126	120	101	104	125	173	200	280
— Relative increase [%]	1.4	1.2	1.1	1.1	1.3	2.0	2.0	3.0
Baseline cost [€]	494	581	553	700	666	464	1106	1746
MPC cost [€]	462	557	536	678	638	417	997	1477
— Savings [€]	32	24	17	22	28	47	109	269
— Relative savings [%]	6.6	4.0	3.1	3.2	4.1	10.1	9.9	15.4
— DHW share of savings [%]	83.4	75.4	71.6	70.4	76.6	81.6	75.9	83.4
Apartment block (AB)								
Baseline consumption [kWh]	84,814	94,639	90,863	94,270	90,174	82,618	95,968	90,281
MPC consumption [kWh]	86,332	96,055	92,101	95,459	91,655	84,478	97,919	92,772
— Increase [kWh]	1517	1416	1238	1189	1481	1859	1951	2491
— Relative increase [%]	1.8	1.5	1.4	1.3	1.6	2.3	2.0	2.8
Baseline cost [€]	4804	5648	5349	6827	6454	4568	10,709	17,272
MPC cost [€]	4433	5381	5153	6578	6137	4049	9462	14,252
— Savings [€]	371	267	196	249	317	519	1247	3020
— Relative savings [%]	7.7	4.7	3.7	3.6	4.9	11.4	11.6	17.5
— DHW share of savings [%]	86	78.7	74.8	74.1	78.8	87.5	78.5	88.0

Table 5. Detailed yearly results per m^2 for the detached house (DH).

Consumption [kWh/m²]		**2015**	**2016**	**2017**	**2018**	**2019**	**2020**	**2021**	**2022**
Heating	Baseline	32.05	39.41	37.06	38.85	36.18	30.07	40.75	36.62
	MPC	31.43	38.78	36.46	38.31	35.54	29.49	40.28	36.38
Cooling	Baseline	0.31	0.40	0.26	0.61	0.46	0.41	0.56	0.50
	MPC	0.32	0.42	0.27	0.62	0.47	0.43	0.58	0.54
DHW	Baseline	32.38	32.35	32.39	32.34	32.36	32.36	32.37	32.36
	MPC	33.91	33.85	33.73	33.62	33.90	34.19	34.29	34.63
Costs [€/m²]									
Heating	Baseline	1.78	2.34	2.13	2.73	2.56	1.57	4.69	6.29
	MPC	1.74	2.30	2.10	2.68	2.51	1.50	4.50	5.97
Cooling	Baseline	0.02	0.02	0.02	0.05	0.03	0.03	0.06	0.13
	MPC	0.02	0.03	0.02	0.05	0.03	0.03	0.06	0.13
DHW	Baseline	1.84	1.92	1.93	2.38	2.31	1.83	3.41	6.45
	MPC	1.64	1.79	1.84	2.27	2.16	1.54	2.80	4.80

Table 6. Detailed yearly results per m^2 for the apartment block (AB).

Consumption [kWh/m²]		**2015**	**2016**	**2017**	**2018**	**2019**	**2020**	**2021**	**2022**
Heating	Baseline	20.09	26.11	23.88	25.71	23.29	18.64	26.81	23.31
	MPC	19.51	25.51	23.34	25.18	22.68	17.98	26.11	22.56
Cooling	Baseline	0.34	0.44	0.29	0.62	0.47	0.43	0.54	0.50
	MPC	0.36	0.46	0.30	0.63	0.49	0.45	0.56	0.55
DHW	Baseline	32.31	32.30	32.33	32.29	32.31	32.30	32.32	32.32
	MPC	33.81	33.77	33.63	33.54	33.82	34.10	34.22	34.58
Costs [€/m²]									
Heating	Baseline	1.13	1.57	1.38	1.82	1.67	0.99	3.20	4.16
	MPC	1.09	1.53	1.35	1.78	1.62	0.95	3.03	3.95
Cooling	Baseline	0.02	0.03	0.02	0.05	0.04	0.03	0.06	0.13
	MPC	0.02	0.03	0.02	0.05	0.04	0.03	0.06	0.12
DHW	Baseline	1.84	1.92	1.93	2.38	2.31	1.83	3.41	6.45
	MPC	1.64	1.79	1.84	2.26	2.16	1.54	2.80	4.80

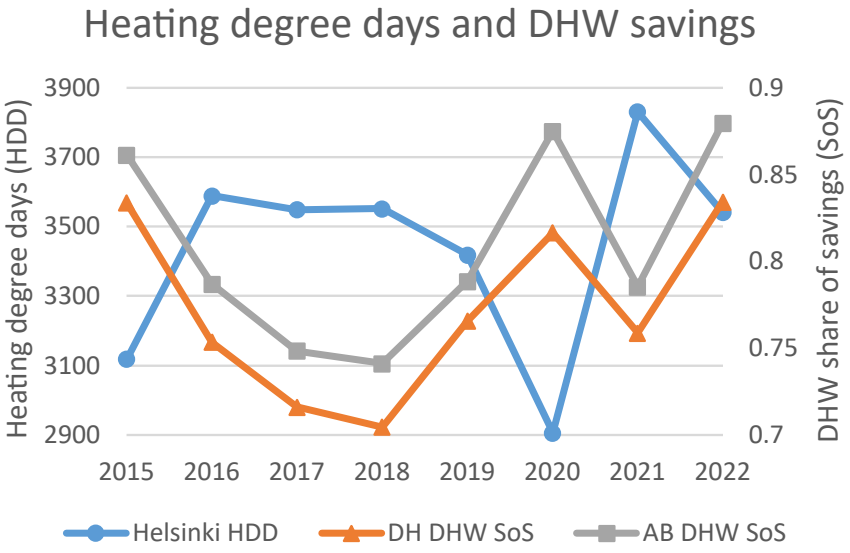

Figure 8. Heating degree days (HDD) in Helsinki [44] compared to the domestic hot water (DHW) share of savings (SoS).

3.2. Impact of Forecast Horizon

Since the results in Section 3.1 used a rather conservative forecast horizon length of 12 h, impacts of increasing it were analysed a bit further. Table 7 presents the relative increase in the achieved cost savings compared to the hourly 12 h horizon cost-optimised MPC with respect to varying the optimisation interval and horizon. Increasing the optimisation horizon to 24 h resulted in a 0.1–1.3% and 0.2–4.6% improvement in yearly savings for the DH and AB, respectively, while increasing it further to 36 h resulted in corresponding 0.1–1.7% and 0.2–7.3% improvements, depending on the simulated year. Even when using a horizon of 8760 h, essentially optimising the full year at one go with perfect information, savings could only be improved by 0.2–3.0% for the DH and by 0.9–9.8% for the AB. Furthermore, using an optimisation horizon of 336 h achieved essentially identical performance, indicating that the buildings either could not effectively store heat for longer than two weeks at most, or that the MPC rarely saw value in such long-term storage. Ultimately, considering that the most yearly savings for the DH and AB were able to achieve were 269 € and 3020 € in 2022, respectively, even the 3.0% and 9.8% increases are not overly significant. It is also worth noting that, in reality, uncertainty in future electricity prices and weather conditions would reduce these additional savings even further.

Table 7. Increases in yearly savings by optimisation interval and horizon relative to the hourly 12 h horizon results presented in Table 4.

Detached House (DH)					**Apartment Block (AB)**				
Interval [h]	**1**	**1**	**168**	**8736**	**Interval [h]**	**1**	**1**	**168**	**8736**
Horizon [h]	**24**	**36**	**336**	**8760**	**Horizon [h]**	**24**	**36**	**336**	**8760**
2022 [%]	1.3	1.7	2.9	3.0	2022 [%]	4.6	7.3	9.8	9.8
2021 [%]	0.8	1.2	2.1	2.1	2021 [%]	3.6	5.9	8.4	8.4
2020 [%]	0.9	1.0	1.7	1.7	2020 [%]	2.7	4.4	6.3	6.5
2019 [%]	0.4	0.4	0.5	0.5	2019 [%]	0.6	0.7	1.5	1.5
2018 [%]	0.2	0.2	0.3	0.3	2018 [%]	0.4	0.6	1.5	1.5
2017 [%]	0.1	0.1	0.2	0.2	2017 [%]	0.2	0.2	0.9	0.9
2016 [%]	0.3	0.3	0.5	0.5	2016 [%]	0.5	0.9	2.2	2.2
2015 [%]	0.6	0.6	0.8	0.8	2015 [%]	0.7	1.1	2.6	2.6

The execution time for the results presented in Table 4 using an hourly 12 h rolling horizon optimisation was around 23 min regardless of the year, with each solve taking less than a second on average. Similarly, for the four optimisation interval and horizon settings presented in Table 7, the execution times from left to right were roughly 24 min, 25 min, 25 s, and 50 s. In principle, Backbone could thus be used for real-time high-level economic MPC, although the presented simplified model lacks the necessary accuracy for actual control applications. Furthermore, while the speed of the full-year simulations could be improved by increasing the optimisation interval, solving optimal control only once a week or year is only possible with perfect information.

4. Discussion

The purpose of this paper was to demonstrate that the large-scale energy system model Backbone captures the essence of simple building-level MPC, facilitating studying the impacts of such MPC on the energy-system scale. Overall, the building-level MPC implemented using the Backbone energy system modelling framework behaved rationally. Given hourly spot electricity price as the control signal, the MPC could be seen to exploit the available flexibility throughout the year in Figure 5, and consumption was observed shifting to hours of cheaper electricity in Figure 6.

In order to ensure the reliability of the desired behaviour, simulations were performed for years between 2015 and 2022, with the results presented in Table 4. The observed relative cost savings compared to the chosen baseline agree with the existing literature [11,45], again lending credence to the applicability of Backbone for capturing impacts of building-level

MPC operations. Furthermore, the increasing volatility of electricity prices in the recent years resulted in increased cost savings from flexibility.

Compared to the DH, the AB achieved slightly better yearly cost savings, likely due to its larger DHW tank. The DHW tank was found to be responsible for roughly three-quarters of the cost savings, despite accounting for only slightly more than half of the total yearly electricity demand as seen in Tables 5 and 6. The duration curves in Figure 7 illustrate that space heating and cooling flexibility was employed on relatively few hours when compared to the DHW tank due to not being economical. Calculating crude estimates for the flexibility of the interior air and DHW tank nodes by multiplying their thermal masses with their permitted temperature ranges suggests that the DHW should account for around 82% of the available flexibility in both buildings, around the same order of magnitude as the achieved savings. While there is considerable thermal mass contained in the structure nodes, their contribution to the space heating flexibility in this case seems minimal. However, this could potentially be improved by using, e.g., underfloor heating, where heat can be more effectively stored in the structural mass of the building. Regardless, the above discussion is highly dependent on the assumed DHW tank sizing and technical properties, and more detailed models for the DHW tank and space heating are recommended in order to properly compare their flexibility.

Curiously, the space heating systems achieved larger shares of the generated savings for the DH than the AB, despite AB being more massive and energy efficient as evidenced by Tables 1, 2, 5 and 6. Similarly, Figure 8 indicates that the space heating systems achieved a larger share of the yearly savings during colder years with more heating demand, despite the increased heat losses from utilising the headroom in the indoor air temperature. It would seem that even though improved energy efficiency should allow for more efficient heat storage for the building interior, the accompanying reduction in the volume of shifted heating demand reduces the total generated savings compared to the DHW tank. However, this is again dependent on the technical properties of the modelled heating systems, and far-reaching conclusions should be left up to future research using more detailed building simulation models.

For practical MPC of buildings, the models used need to be able to run as often as there are meaningful updates to the input data. In the NordPool power exchange for example, the market is cleared once a day between 12:00 and 13:00 CET, determining the area prices for the next day. As a result, depending on the time of day, an MPC has anywhere between 12 and 36 h of known future electricity prices. However, while the electricity prices might update only once every 24 h, ambient conditions and occupancy in the building in question are in a constant flux, requiring more frequent evaluation of the predicted optimal control. The results using different optimisation intervals and horizons presented in Table 7 reflect this fact, with the results using an hourly interval simulating as close to real-time operation as possible with the used hourly time series data.

Looking at the results presented in Table 7, Backbone was able to achieve greater savings when the length of the optimisation horizon was increased. The magnitude of the improvements for the AB in particular were somewhat surprising in 2020–2022, although perfect information was used for simplicity. Typically, the existing literature on building-level economic MPC tends to focus on horizons between 12 and 36 h as determined by existing electricity market structures [10,46], but for buildings with large DHW tanks and considerable thermal mass, it seems that such horizons might not be sufficient for capturing all the benefits of the inherent thermal storage capacity. That said, the additional savings achieved with horizons beyond 36 h were practically negligible. Furthermore, in reality, as the length of the optimisation horizon increases, it becomes increasingly difficult to obtain good quality forecasts on future electricity prices, weather conditions, and occupant behaviour. Without good quality forecasts, the MPC risks making mistakes, reducing the amount of achieved savings. While employing either robust or stochastic optimisation could help mitigate the forecast-related risks, these methods also impact the expected

savings. Lastly, increasing the length of the optimisation horizon inevitably also increases the computational time to solve each interval.

5. Conclusions

Overall, the performance of the building-level MPC implemented using the Backbone energy system optimisation framework was deemed reasonable. Given no incentive to utilise the flexibility in the space heating/cooling and water heating demands by providing the model with constant electricity prices, the model simply took minimum action necessary to maintain the required indoor air and DHW tank temperatures. On the other hand, minimising electricity costs against hourly spot prices resulted in utilising the thermal storage capacity inherent in the DHW tanks and building thermal mass to shift consumption to hours of cheap electricity. Furthermore, the resulting cost savings around 3.1–17.5% agree with comparable values found in the literature [11,45] and could be seen to increase in the recent years of 2020–2022 at least partly due to increased volatility in electricity prices. The impact of the used forecast horizon was deemed quite insignificant beyond the maximum day-ahead market horizon of 36 h ahead of time.

The DHW tanks were found responsible for roughly three-quarters of the cost savings, despite only accounting for slightly over half of the yearly electricity consumption. However, the simplified modelling approach used in this work could distort the results one way or the other, and more detailed models should be employed for a conclusive comparison. Furthermore, the flexibility of space heating could potentially be improved with different heat distribution systems or by temporarily falling to a set-back temperature if the situation allows. Regardless, DHW tanks seem capable of offering considerable flexibility with comparatively low practical complexity.

While this work focused on cost savings on the level of individual buildings for demonstration and validation purposes, the used approach has been designed primarily for energy-system scales required to quantify the system-level cost savings related to, e.g., variable renewable energy integration and peak load reduction. Based on the presented results, integrating simplified building MPC into large-scale energy system modelling frameworks such as Backbone seems to be a reasonable approach for studying the impacts of widespread building-scale DSM on the operation of the overarching energy system. However, further research is required to compare building-level energy flexibility on an equal footing with grid-scale solutions in capacity expansion models.

Author Contributions: Conceptualisation, T.R., T.L., A.H. and R.R.; Data curation, T.R. and T.L.; Formal analysis, T.R. and T.L.; Funding acquisition, A.H. and J.K.; Investigation, T.R. and T.L.; Methodology, T.R. and T.L.; Project administration, A.H. and J.K.; Resources, A.H. and J.K.; Software, T.R. and T.L.; Supervision, A.H.; Validation, T.R. and T.L.; Visualisation, T.R. and T.L.; Writing—original draft, T.R., T.L. and R.R.; Writing—review and editing, T.R., T.L., A.H., R.R. and J.K. All authors have read and agreed to the published version of the manuscript.

Funding: This research was funded by the Academy of Finland project *Integration of building flexibility into future energy systems (FlexiB)* under grant agreements No. 332421 and 333364.

Data Availability Statement: The raw data, results, as well as the code used for processing the data for the simulations have been made available through Zenodo [29].

Conflicts of Interest: The authors declare no conflict of interest. Furthermore, the funding agency had no role in the design of the study; in the collection, analyses, or interpretation of data; in the writing of the manuscript; or in the decision to publish the results.

Abbreviations

The following abbreviations are used in this manuscript:

AB	Apartment block
DH	Detached house

DHW	Domestic hot water
DSM	Demand-side management
G2WHP	Ground-to-water heat pump
HDD	Heating degree day
HVAC	Heating, ventilation, and air conditioning
MILP	Mixed-integer linear programming
MPC	Model-predictive control
RC	Resistance–capacitance
SPF	Seasonal performance factor

References

1. International Energy Agency (IEA). *Buildings—Sectorial Overview*; International Energy Agency (IEA): Paris, France, 2022. Available online: https://www.iea.org/energy-system/buildings (accessed on 2 February 2023).
2. Global Alliance for Buildings and Construction; International Energy Agency; United Nations Environment Programme. *2019 Global Status Report for Buildings and Construction: Towards a Zero-Emission, Efficient and Resilient Buildings and Construction Sector*; Technical report; International Energy Agency: Paris, France, 2019. Available online: https://www.iea.org/reports/global-status-report-for-buildings-and-construction-2019 (accessed on 31 October 2023).
3. Eurostat. *Statistics Explained — Energy Consumption in Households*; Eurostat: Luxembourg, 2022. Available online: https://ec.europa.eu/eurostat/statistics-explained/index.php?title=Energy_consumption_in_households (accessed on 2 February 2023)
4. Bloess, A.; Schill, W.P.; Zerrahn, A. Power-to-heat for renewable energy integration: A review of technologies, modeling approaches, and flexibility potentials. *Appl. Energy* **2018**, *212*, 1611–1626. [CrossRef]
5. Péan, T.Q.; Salom, J.; Costa-Castelló, R. Review of control strategies for improving the energy flexibility provided by heat pump systems in buildings. *J. Process. Control.* **2019**, *74*, 35–49. [CrossRef]
6. Zong, Y.; Su, W.; Wang, J.; Rodek, J.K.; Jiang, C.; Christensen, M.H.; You, S.; Zhou, Y.; Mu, S. Model predictive control for smart buildings to provide the demand side flexibility in the multi-carrier energy context: Current status, pros and cons, feasibility and barriers. In Proceedings of the 10th International Conference on Applied Energy ICAE2018, Hong Kong, China, 22–25 August 2018; Elsevier: Amsterdam, The Netherlands, 2019; pp. 3026–3031. [CrossRef]
7. Drgoňa, J.; Arroyo, J.; Cupeiro Figueroa, I.; Blum, D.; Arendt, K.; Kim, D.; Ollé, E.P.; Oravec, J.; Wetter, M.; Vrabie, D.L.; et al. All you need to know about model predictive control for buildings. *Annu. Rev. Control.* **2020**, *50*, 190–232. [CrossRef]
8. Kathirgamanathan, A.; De Rosa, M.; Mangina, E.; Finn, D.P. Data-driven predictive control for unlocking building energy flexibility: A review. *Renew. Sustain. Energy Rev.* **2021**, *135*, 110120. [CrossRef]
9. Lee, J.H. Model predictive control: Review of the three decades of development. *Int. J. Control. Autom. Syst.* **2011**, *9*, 415–424. [CrossRef]
10. Yao, Y.; Shekhar, D.K. State of the art review on model predictive control (MPC) in Heating Ventilation and Air-conditioning (HVAC) field. *Build. Environ.* **2021**, *200*, 107952. [CrossRef]
11. Taheri, S.; Hosseini, P.; Razban, A. Model predictive control of heating, ventilation, and air conditioning (HVAC) systems: A state-of-the-art review. *J. Build. Eng.* **2022**, *60*, 105067. [CrossRef]
12. Halvgaard, R.; Poulsen, N.K.; Madsen, H.; Jørgensen, J.B. Economic Model Predictive Control for building climate control in a Smart Grid. In Proceedings of the 2012 IEEE PES Innovative Smart Grid Technologies (ISGT), Washington, DC, USA, 16–20 January 2012; pp. 1–6. [CrossRef]
13. Ma, J.; Qin, J.; Salsbury, T.; Xu, P. Demand reduction in building energy systems based on economic model predictive control. *Chem. Eng. Sci.* **2012**, *67*, 92–100. [CrossRef]
14. West, S.R.; Ward, J.K.; Wall, J. Trial results from a model predictive control and optimisation system for commercial building HVAC. *Energy Build.* **2014**, *72*, 271–279. [CrossRef]
15. Ruusu, R.; Cao, S.; Manrique Delgado, B.; Hasan, A. Direct quantification of multiple-source energy flexibility in a residential building using a new model predictive high-level controller. *Energy Convers. Manag.* **2019**, *180*, 1109–1128. [CrossRef]
16. Vand, B.; Ruusu, R.; Hasan, A.; Manrique Delgado, B. Optimal management of energy sharing in a community of buildings using a model predictive control. *Energy Convers. Manag.* **2021**, *239*, 114178. [CrossRef]
17. Bach, B.; Werling, J.; Ommen, T.; Münster, M.; Morales, J.M.; Elmegaard, B. Integration of large-scale heat pumps in the district heating systems of Greater Copenhagen. *Energy* **2016**, *107*, 321–334. [CrossRef]
18. Salpakari, J.; Mikkola, J.; Lund, P.D. Improved flexibility with large-scale variable renewable power in cities through optimal demand side management and power-to-heat conversion. *Energy Convers. Manag.* **2016**, *126*, 649–661. [CrossRef]
19. Hedegaard, K.; Balyk, O. Energy system investment model incorporating heat pumps with thermal storage in buildings and buffer tanks. *Energy* **2013**, *63*, 356–365. [CrossRef]
20. Hedegaard, K.; Münster, M. Influence of individual heat pumps on wind power integration—Energy system investments and operation. *Energy Convers. Manag.* **2013**, *75*, 673–684. [CrossRef]
21. Cooper, S.J.; Hammond, G.P.; McManus, M.C.; Pudjianto, D. Detailed simulation of electrical demands due to nationwide adoption of heat pumps, taking account of renewable generation and mitigation. *IET Renew. Power Gener.* **2016**, *10*, 380–387. [CrossRef]

22. Arteconi, A.; Patteeuw, D.; Bruninx, K.; Delarue, E.; D'haeseleer, W.; Helsen, L. Active demand response with electric heating systems: Impact of market penetration. *Appl. Energy* **2016**, *177*, 636–648. [CrossRef]
23. Rasku, T.; Kiviluoma, J. A Comparison of Widespread Flexible Residential Electric Heating and Energy Efficiency in a Future Nordic Power System. *Energies* **2018**, *12*, 5. [CrossRef]
24. Huckebrink, D.; Bertsch, V. Decarbonising the residential heating sector: A techno-economic assessment of selected technologies. *Energy* **2022**, *257*, 124605. [CrossRef]
25. Kröger, D.; Peper, J.; Rehtanz, C. Electricity market modeling considering a high penetration of flexible heating systems and electric vehicles. *Appl. Energy* **2023**, *331*, 120406. [CrossRef]
26. Ringkjøb, H.K.; Haugan, P.M.; Solbrekke, I.M. A review of modelling tools for energy and electricity systems with large shares of variable renewables. *Renew. Sustain. Energy Rev.* **2018**, *96*, 440–459. [CrossRef]
27. Li, X.; Wen, J. Review of building energy modeling for control and operation. *Renew. Sustain. Energy Rev.* **2014**, *37*, 517–537. [CrossRef]
28. Li, Y.; O'Neill, Z.; Zhang, L.; Chen, J.; Im, P.; DeGraw, J. Grey-box modeling and application for building energy simulations—A critical review. *Renew. Sustain. Energy Rev.* **2021**, *146*, 111174. [CrossRef]
29. Rasku, T. *FlexiB Spine Toolbox Workflow for Backbone Model-Predictive Control Data*; Zenodo: Geneva, Switzerland, 2023. . [CrossRef]
30. EQUA. *IDA Early Stage Building Optimization (ESBO)*, v1.13; EQUA: Solna, Sweden, 2013.
31. Finnish Ministry of the Environment. *D3 Rakennusten Energiatehokkuus—Määräykset ja Ohjeet 2012 (D3 Energy Efficiency of Buildings—Regulations and Guidelines 2012)*; Finnish Ministry of the Environment: Helsinki, Finland, 2011. Available online: https://ym.fi/documents/1410903/0/37188-D3-2012_Suomi.pdf/3072837e-928a-424c-f7dc-b6b61f7b8da6/37188-D3-2012_Suomi.pdf?t=1622704540584 (accessed on 30 March 2023).
32. Rasku, T.; Simson, R.; Kiviluoma, J. *Sensitivity of a Simple Lumped-Capacitance Building Thermal Modelling Approach Intended for Building-Stock-Scale Flexibility Studies*; Preprint; Zenodo: Geneva, Switzerland, 2023. [CrossRef]
33. Chong, A.; Gu, Y.; Jia, H. Calibrating building energy simulation models: A review of the basics to guide future work. *Energy Build.* **2021**, *253*, 111533. [CrossRef]
34. Finnish Ministry of the Environment. *Ympäristöministeriön Asetus Uuden Rakennuksen Sisäilmastosta ja Ilmanvaihdosta (Ministry of the Environment Statute on the Indoor Climate and Ventilation of New Buildings*); Finnish Ministry of the Environment: Helsinki, Finland, 2017. https://finlex.fi/fi/laki/alkup/2017/20171009.
35. Kurnitski, J.; Kalliomäki, P.; Haakana, M.; Shemeikka, J.; Laitininen, A.; Krzysztof, K.; Saari, M.; Kukkonen, P. *Lämmitysjärjestelmät ja Lämmin Käyttövesi—Laskentaopas (Heating Systems and Domestic Hot Water—Calculation Guide)*; Finnish Ministry of the Environment: Helsinki, Finland, 2011. Available online: https://ym.fi/documents/1410903/38439968/Lammitysjarjestelmat-_Laskentaopas-2012-150911-CA99FFCB_627B_48C8_8EB0_607F36B178A5-30751.pdf/a2f589d0-47ac-5d04-b739-759b514e2245/Lammitysjarjestelmat-_Laskentaopas-2012-150911-CA99FFCB_627B_48C8_8EB0_607F36B178A5-30751.pdf?t=1603260210304 (accessed on 30 March 2023).
36. Eskola, L.; Jokisalo, J.; Sirén, K. *Lämpöpumppujen Energialaskentaopas (Energy Calculation Guide for Heat Pumps)*; Finnish Ministry of the Environment: Helsinki, Finland, 2012. Available online: https://ym.fi/documents/1410903/38439968/Lampopumppujen-energialaskentaopas-3.10.2012-10A732A6_EA2F_45F9_869C_6F909138CB26-30757.pdf/1d053cd5-1865-e174-6424-841fac831c48/Lampopumppujen-energialaskentaopas-3.10.2012-10A732A6_EA2F_45F9_869C_6F909138CB26-30757.pdf?t=1603260214849 (accessed on 24 March 2023).
37. Rasku, T. *ArchetypeBuildingModel.jl*, Version 2.1.3; GitHub: San Francisco, CA, USA; Zenodo: Geneva, Switzerland, 2022. [CrossRef]
38. Hofmann, F.; Hampp, J.; Neumann, F.; Brown, T.; Hörsch, J. atlite: A Lightweight Python Package for Calculating Renewable Power Potentials and Time Series. *J. Open Source Softw.* **2021**, *6*, 3294. [CrossRef]
39. Hersbach, H.; Bell, B.; Berrisford, P.; Hirahara, S.; Horányi, A.; Muñoz-Sabater, J.; Nicolas, J.; Peubey, C.; Radu, R.; Schepers, D.; et al. The ERA5 global reanalysis. *Q. J. R. Meteorol. Soc.* **2020**, *146*, 1999–2049. [CrossRef]
40. Helistö, N.; Kiviluoma, J.; Ikäheimo, J.; Rasku, T.; Rinne, E.; O'Dwyer, C.; Li, R.; Flynn, D. Backbone—An Adaptable Energy Systems Modelling Framework. *Energies* **2019**, *12*, 3388. [CrossRef]
41. ENTSO-E. Central Collection And Publication Of Electricity Generation, Transportation and Consumption Data and Information for the Pan-European Market. Available online: https://transparency.entsoe.eu/transmission-domain/r2/dayAheadPrices/show (accessed on 10 January 2023).
42. Finnish Tax Administration. Tax Rates on Electricity and Certain Fuels. Available online: https://www.vero.fi/en/businesses-and-corporations/taxes-and-charges/excise-taxation/sahkovero/Tax-rates-on-electricity-and-certain-fuels/ (accessed on 5 January 2023).
43. Forrest, J.; Ralphs, T.; Santos, H.G.; Vigerske, S.; Forrest, J.; Hafer, L.; Kristjansson, B.; jpfasano; Straver, E.; Lubin, M.; et al. *coin-or/Cbc*; GitHub: San Francisco, CA, USA; Zenodo: Geneva, Switzerland, 2022. [CrossRef]
44. Finnish Meteorological Institute (FMI). Heating Degree Days. Available online: https://en.ilmatieteenlaitos.fi/heating-degree-days (accessed on 27 March 2023).

45. Kim, D.; Lee, J.; Do, S.; Mago, P.J.; Lee, K.H.; Cho, H. Energy Modeling and Model Predictive Control for HVAC in Buildings: A Review of Current Research Trends. *Energies* **2022**, *15*, 7231. [CrossRef]
46. Afram, A.; Janabi-Sharifi, F. Theory and applications of HVAC control systems—A review of model predictive control (MPC). *Build. Environ.* **2014**, *72*, 343–355. [CrossRef]